Mitochondrion 12 (2012) 630–639

Contents lists available at SciVerse ScienceDirect

Mitochondrion

journal homepage: www.elsevier.com/locate/mito

Pifithrin-μ increases mitochondrial COX biogenesis and MnSOD activity in skeletal muscle of middle-aged mice

Jie He [a,b,1], Zhengtang Qi [a,b,1], Yuhui Su [a], Qiang He [a], Jingxia Liu [a], Lu Yu [a], Omar S. Al-Attas [c], Tajamul Hussain [c], Edgardo Tan De Rosas [d], Liu Ji [a,b], Shuzhe Ding [a,b,*]

[a] Key Laboratory of Adolescent Health Assessment and Exercise Intervention, Ministry of Education, Shanghai 200241, China
[b] College of Physical Education and Health, East China Normal University, Shanghai 200241, China
[c] Center of Excellence in Biotechnology Research, King Saud University, Riyadh 11451, Saudi Arabia
[d] Department of Biochemistry, King Saud University, Riyadh 11451, Saudi Arabia

ARTICLE INFO

Article history:
Received 24 November 2011
Received in revised form 28 August 2012
Accepted 13 September 2012
Available online 21 September 2012

Keywords:
Skeletal muscle
p53
Mitochondrial biogenesis
Pifithrin
MnSOD
Cytochrome c oxidase

ABSTRACT

We investigated the biogenesis and mitochondrial antioxidant capacity of cytochrome c oxidase (COX) within the skeletal muscle under the treatments of p53 inhibitors (pifithrin, PFTα and PFTμ). Significantly, PFTμ increased mtDNA content and COX biogenesis. These changes coincided with increases in the activity and expression of manganese superoxide dismutase (MnSOD), the key antioxidant enzyme in mitochondria. Conversely, PFTα caused muscle loss, increased oxidative damage and decreased MnSOD activity in intermyofibrillar (IMF) mitochondria. Mechanically, PFTμ inhibited p53 translocation to mitochondria and thus increased its transcriptional activity for expression of synthesis of cytochrome c oxidase 2 (SCO2), an important assembly protein for COX. This study provides in vivo evidence that PFTμ, superior to PFTα, preserves muscle mass and increases mitochondrial antioxidant activity.

1. Introduction

p53 is a key regulator that functions by transcription-dependent or -independent pathways in the cell. In vitro, p53 controls cellular oxidative stress and mitochondrial biogenesis by the two pathways. Synthesis of cytochrome c oxidase (SCO) 2 and TIGAR (TP53-induced glycolysis and apoptosis regulator) have been identified as p53-inducible genes. SCO (SCO1, SCO2) is critical for controlling cellular copper homeostasis and assembling the complex of cytochrome c oxidase (COX) during holoenzyme biogenesis (Leary, 2010; Leary et al., 2007). TIGAR expression lowers fructose-2,6-bisphosphate levels in cells, resulting in an inhibition of glycolysis and an overall decrease in reactive oxygen species (ROS) levels (Bensaad et al., 2006). Overall, p53 regulates redox state, ATP-generating pathway, mitochondrial biogenesis and respiration via the transcriptional target SCO2 and TIGAR (Kruse and Gu, 2006; Leary, 2010; Matoba et al., 2006). By the transcription-independent pathway, p53 interacts with the mitochondrial transcription factor A (TFAM) in mitochondria, and thus regulates mtDNA content (Park et al., 2009). Binding of TFAM to DNA is significantly enhanced by p53, so the physical interaction of p53 with TFAM plays an important role in mtDNA replication and transcription (Yoshida et al., 2003). Manganese superoxide dismutase (MnSOD) is a p53-regulated gene that is a vital antioxidant enzyme localized in the matrix of mitochondria by scavenging ROS. p53 affects mitochondrial ROS production, in part, by regulating the expression of MnSOD (Dhar et al., 2006; Holley et al., 2010a). In the mitochondria, p53 can interact physically with MnSOD and reduce its superoxide scavenging activity, resulting in a subsequent decrease in mitochondrial membrane potential (Zhao et al., 2005). Additionally, p53 serves as an exonuclease in cell and may be a component of a DNA error-repair pathway (Mummenbrauer et al., 1996). In the cytoplasm p53 also exerts 3′→5′ exonuclease activity with dsRNA. The dsRNase activity of p53 in the cytoplasm plays a possible role in the inhibition of translation and induction of apoptosis (Grinberg et al., 2010). The activation of p53 is primarily mediated by post-translational modifications that affect its conformation and capacity to bind to several proteins, resulting in its stabilization and enhanced DNA-binding potential. The role of p53 in the cell depends on the regulation of p53 activity by its intracellular distribution (Wesierska-Gadek and Schmid, 2005).

Pifithrin-α (PFT-α) is a reversible inhibitor of p53-mediated apoptosis and p53-dependent gene transcription (Farah et al., 2007). PFT-α blocks the transcriptional activity of p53 specifically, and therefore is used to prevent the severe side effects associated with chemo- and

* Corresponding author at: College of Physical Education and Health, East China Normal University, No. 500 Dongchuan Road, Minhang District, Shanghai 200241, China. Tel./fax: +86 21 54345296.
E-mail address: szding@tyxx.ecnu.edu.cn (S. Ding).
[1] Jie He and Zhengtang Qi contributed equally to this work.

1567-7249/$ – see front matter © 2012 Elsevier B.V. and Mitochondria Research Society. All rights reserved.
http://dx.doi.org/10.1016/j.mito.2012.09.003

radiotherapy (Sohn et al., 2009). PFT-α may specifically inhibit p53 signaling after p53 translocation to the nucleus (Murphy et al., 2004). PFT-μ is an inhibitor of p53 binding and is anti-apoptotic, as PFT-μ directly inhibits p53 binding to mitochondria as well as to Bcl-xL and Bcl-2 proteins (Hagn et al., 2010). PFT-μ not only inhibits mitochondrial release of cytochrome c, but also inhibits oxidative stress. Unexpectedly, PFT-μ also inhibited hypoxic–ischemic-induced upregulation of p53 target genes, such as PUMA and Noxa. The neuroprotective effect of inhibiting only p53 transcriptional activity by PFT-α was significantly smaller and did not involve reduced oxidative stress. As a consequence, targeting p53 mitochondrial translocation by PFT-μ develops into a novel and powerful neuroprotective strategy (Nijboer et al., 2011). PFT-μ not only shuts down the p53-mitochondrial pathway but also affects the transcriptional functions of p53, so it is considered superior to PFT-α for improving p53 activity. For example, nutlin is a selective pharmacological MDM2 inhibitor that binds to the p53-binding pocket, thereby leading to apoptosis pathways. Specific inhibition of mitochondrial p53 translocation by PFT-μ reduces the apoptotic response to nutlin by 2.5-folds, underlining the significance of p53's mitochondrial program in nutlin-induced apoptosis in tumor cells. However, the p53-specific transcriptional inhibitor PFT-α, not only fails to inhibit, but greatly potentiates nutlin-induced apoptosis (Vaseva et al., 2009). In multiple myeloma, PFT-α, not only inhibited nutlin-induced upregulation of p53-transcriptional targets but also augmented apoptosis, suggesting an association of the transcription-independent pathway of apoptosis. However, PFT-μ did not prevent nutlin-induced apoptosis, suggesting that the p53 transcription-dependent pathway was also operational in nutlin-induced apoptosis (Saha et al., 2010).

Despite considerable interest in the pharmacological effects of pifithrin in cancer therapy and the molecular effects of pifithrin in apoptosis, the findings are less consistent, and studies on the effects on skeletal muscle are especially absent. In addition, it is evident for p53 to play a multiple role in regulating mitochondrial function, cell cycle, apoptosis and autophagy. Thus, inhibition of p53 activity in a single pathway may result in an unknown outcome. Herein, we hypothesize that pifithrin changes the mitochondrial redox state and COX biogenesis and assembly in skeletal muscle for p53 roles in ROS scavenging and SCO2 expression. Middle-aged mice are employed to assess the effects of PFT-μ, compared to PFT-α. We aim to explore the effects of pifithrin on antioxidant capacity in mitochondrial subfractions and expression of genes controlling the biogenesis and assembly of the COX complex in the skeletal muscle, and ChIP and Co-IP assays are used to further elucidate the underlying mechanisms related to the p53-mitochondrial pathway.

2. Materials and methods

2.1. Animals

Male ICR/CD-1 mice were purchased from Sino-British Sippr/BK Lab Animal Ltd., Co. (Shanghai, China) at 8–9 months of age (middle-aged), and were housed at East China Normal University until sacrifice. PFTα (Sigma, 63208-82-2) and PFTμ (Sigma, 64984-31-2) were dissolved in DMSO/saline (1:9 v/v). The mice received intraperitoneal injection of PFTμ or PFTα (3 mg/kg body weight/2 days) for 3 weeks. The vehicle (10% DMSO in saline) was injected as a sham treatment for mice that were not treated with PFT. All animals were housed in a temperature (21 ± 2 °C) and light-controlled (12:12 h light–dark cycle) environment, and were provided food and water ad libitum. Following approval by the local government, all experiments were performed in accordance with the guidelines for the use of laboratory animals published by the China Ministry of Health (No. 55 order, ordained on 25 Jan, 1998). All experimental procedures were approved by the Experimental Animal Care and Use Committee at East China Normal University (ECNU 2006-05).

2.2. Tissue extraction and mitochondrial isolation

Upon sacrifice, the gastrocnemius, EDL and quadriceps were removed, rinsed in PBS solution, and dried with filter paper; fresh tissue (gastrocnemius) was used for mitochondrial isolation. The other muscles were frozen in liquid nitrogen, and stored at −80 °C. Subsarcolemmal (SS) and intermyofibrillar (IMF) mitochondria were prepared using modifications of the procedures published previously (Cogswell et al., 1993). Briefly, extracted muscles were placed in buffer 1 (100 mM KCl, 50 mM Tris-base, 5 mM $MgSO_4$ and 5 mM EDTA, pH 7.4, 4 °C). Then, the muscles were minced and diluted in buffer 2 (buffer 1, supplemented with 1 mM ATP) at 4 °C. Thereafter, muscle samples were homogenized briefly using a polytron at 1500 r.p.m. for 10 s at 4 °C. Subsequently the mitochondria were isolated by centrifugation at 800 *g* for 10 min at 4 °C. The resultant supernatant and pellet fractions were used to obtain SS and IMF mitochondria, respectively, as described previously (Yoshida et al., 2007). In order to remove contaminating subcellular materials, the resultant SS and IMF mitochondria were further purified using a 60% Percoll gradient as described previously (Campbell et al., 2004). Mitochondrial protein content was assayed using BSA as a standard according to Bradford.

2.3. Assays of mitochondrial COX activity and oxidative stress

The purified SS and IMF mitochondria were used to measure COX activity and oxidative stress. For COX activity assays, the assay buffer contained 50 mM phosphate buffer, pH 7.0, 0.1% BSA, 0.2% Tween-20, and 40 μM reduced cytochrome c. The reaction was initiated by addition of 3 μg/ml mitochondria and optical density was measured at 550 nm for 2 min (Sun et al., 2010). To assay lipid peroxidation (LPO), MDA levels were measured by the thiobarbituric acid method using a kit (Jiancheng Biotech Inc., Nanjing, China). Reduced glutathione (GSH) content was determined in mitochondria using the commercially available glutathione (GSH) detection kit (Jiancheng Biotech Inc., Nanjing, China) using an assay based on the reaction with the thiol-specific reagent dithionitrobenzoic acid. The adduct was measured spectrophotometrically at 412 nm with a plate reader. A commercially available kit (Jiancheng Biotech Inc., Nanjing, China) was used to measure the MnSOD activity in the purified mitochondria. The assay was performed in a 96-well plate with each sample being treated with and without 10 μl of 12 mM potassium cyanide. Potassium cyanide was used to inhibit CuZnSOD, resulting in the detection of the MnSOD activity only. The reagents and samples were protected from white light and incubated at 26 °C for 20 min with periodic shaking. The absorbance was measured at 450 nm using a 96-well plate reader (Ryan et al., 2010).

2.4. Real-time PCR and mtDNA content assay

Total RNA was prepared from ~100 mg of frozen tissues using TRIzol (Invitrogen, Chromos, Singapore) and purified according to the instructions included. Double-stranded cDNA was synthesized from ~1 μg of total RNA using a ReverTra Ace® qPCR RT kit (TOYOBO, Osaka, Japan). Real-time PCR reactions were set up using the SYBR-Green PCR kit (TOYOBO, Osaka, Japan) and were cycled in a StepOne™ Real-Time PCR System (Applied Biosystems, CA, USA). In brief, RNA concentrations were estimated by measuring the absorbance at 260 nm, and purity was assessed by 260 nm/280 nm absorbance ratio. Total RNA was denatured at 65 °C for 5 min, cooled immediately on ice, and reverse transcribed. The reaction was assessed at 37 °C for 15 min and at 98 °C for 5 min. PCR was performed in a fluorescence temperature cycler containing 4 pmol of each primer, 2.0×Master SYBR Green I (containing Taq DNA polymerase, reaction buffer, dNTP mix, SYBR Green I dye, and 10 mM $MgCl_2$), and 2.0 μl template in a total volume of 20 μl. The amplification occurred in a three-step cycle (denaturation at 95 °C for 15 s, annealing at 61 °C for 30 s, extension and data

collection at 72 °C for 45 s) for 40 cycles. The fluorescence signal was plotted against the cycle number for all samples and external standards. The abundance of the target mRNA was normalized to that of β-actin. Mitochondrial DNA content was determined by real-time PCR. Briefly, total DNA was extracted and purified from muscles. Ten nanograms of DNA was used to quantify mitochondrial and nuclear DNA markers. β-Actin was also used as a nuclear DNA marker. AK140265 was used as mtDNA markers. PCR was performed as stated above. Primer pairs were designed based on GenBank reference sequences and listed in Table S1.

2.5. Western blotting

The isolated muscle tissue (~200 mg) was weighed and cut into pieces at 4 °C, and 2 ml (10×dry weight of isolated muscle fibers) of ice-cold buffer (50 mM Tris HCl, 150 mM NaCl, 1 mM EDTA, 0.2 mM PMSF, 1% NP-40, pH 7.4, Cocktail) was added. The tissue pieces were then homogenized, after which homogenates were centrifuged for 10 min at 8000 *g* and 4 °C. The total protein content of the supernatant was quantified using bicinchoninic acid reagents and BSA standards (Shanghai Sangon, Shanghai, China). The protein samples were diluted in 5×SDS buffer to the same concentration (~2 g/l), boiled for 5 min at 100 °C, and stored at −80 °C. Equal amounts of protein (30 μg/lane) were run on 10% or 12% SDS-polyacrylamide (120 V; Bio-Rad, Miniprotein 3), and proteins were transferred (1 h, 1.2 mA/cm^2, Criterion blotter; Bio-Rad) to PVDF membranes. After Ponceau S staining and destaining, membranes were blocked in 5% nonfat dry milk powder (Shanghai Sangon, Shanghai, China) in Tris-buffered saline containing 0.1% Tween 20 (TBST) for 1–1.5 h at room temperature. Thereafter, a 1:200 dilution of the specific primary antibody (Santa Cruz, Table S2) in 5% TBST was added and incubated overnight at 4 °C on a shaker. After the membranes were washed 3 times for 10, 10, and 10 min in 5% TBST, the membranes were incubated with a 1:1000 dilution of the horseradish peroxidase-conjugated secondary antibody in 5% TBST for 2 h at room temperature. Thereafter, the membranes were washed in TBST for 10 min. Visualization of reaction bands was performed by 3,3′-diaminobenzidine staining (Shanghai Sangon, Shanghai, China) and scanned densitometrically. β-Actin was used to standardize for the amount of protein loaded.

2.6. ChIP assays

ChIP assay was performed using a kit from Upstate Cell Signaling Solutions as described previously (Smith et al., 2007). In brief, chromatin was sheared to fragments by 8–10×15 s bursts of sonication. Following centrifugation (13,000 *g* for 10 min at 4 °C), 100 μl of supernatant, containing chromatin fragments, was diluted 10-folds in a buffer (0.01% SDS, 1.1% Triton X-100, 1.2 mM EDTA, 16.7 mM TrisHCl, and 167 mM NaCl), precleared with salmon sperm DNA/protein A agarose (Upstate #16-157), and centrifuged again (1000 *g* for 1 min at 4 °C). The resultant supernatant, referred to as input sample, was immunoprecipitated with p53 antibody and protein A agarose. Following centrifugation, the protein A agarose/antibody/histone complex was washed for 3–5 min on a rotating platform with 1 ml of each of the buffers listed in the order as given below: low salt immune complex wash buffer; high salt immune complex wash buffer; LiCl immune complex wash buffer; 1×TE (two washes). The pellets were eluted in a buffer consisting of 1% SDS and 0.1 M $NaHCO_3$ and reverse cross-linked by adding 5 M NaCl followed by incubation at 65 °C for 4 h. The coimmunoprecipitated DNA was purified by phenol–chloroform extraction and resuspended in 20 μl H_2O. A fragment corresponding to nucleotides of the mouse SCO2/PUMA/Bax promoter, containing the p53 binding site, was amplified and quantified by qPCR as described above using the +ve primers. A pair of primers (−ve primers) specific to a region downstream from the start site was used as a negative control for nonspecific binding of chromatin to the immuno-precipitation antibody. Purified DNA from the input sample that did not undergo immuno-precipitation was PCR amplified and used to normalize signals from ChIP assays. The DNA content in these control reactions was 1% of those used in parallel immuno-precipitation reactions. A PCR reaction using equal genomic DNA was also run with each set of PCR reactions to allow comparison between different experiments.

2.7. Co-immunoprecipitation

p53 immunoreactivity precipitated by Bcl-XL on the mitochondria was determined by use of previously published methods (Drake et al., 2010). Briefly, muscle was homogenized in a CHAPS-containing buffer [40 mM HEPES (pH 7.5), 120 mM NaCl, 1 mM EDTA, 10 mM pyrophosphate, 10 mM β-glycerophosphate, 40 mM NaF, 1.5 mM sodium vanadate, 0.3% CHAPS, 0.1 mM PMSF, 1 mM benzamidine, and 1 mM DTT], and the homogenate was mixed on a platform rocker for 20 min at 4 °C and then clarified by centrifugation at 1000 *g* for 3 min at 4 °C. Bcl-XL was immunoprecipitated from the supernatant fraction using a monoclonal anti-Bcl-XL antibody. Proteins in the immune complexes were resolved by SDS-PAGE and subjected to Western blot analysis for p53, and Bcl-XL. The ratio of p53 to Bcl-XL was calculated and expressed as the percentage of the lean control value.

2.8. Statistical analysis

Data are reported as mean±SEM. Statistical analysis was performed using Microsoft Excel 2007. Statistical differences between treatments were determined using ANOVA as appropriate. For all tests the significance level was set at $P<0.05$.

3. Results

3.1. MnSOD expression and its activity in mitochondria

Mitochondria are central to redox homeostasis, produce energy, and trigger apoptosis and senescence: not surprisingly, many functions of p53 appear to be based in mitochondria. p53 orchestrates mitochondrial redox signaling by the control of the superoxide scavenger MnSOD (Pani and Galeotti, 2011). Assays in SS mitochondria demonstrated that PFTμ increased MnSOD activity ($P<0.05$), whereas PFTα did not affect MnSOD activity (Fig. 1A). Assays in IMF mitochondria showed that PFTμ had no effect on MnSOD activity, whereas PFTα decreased MnSOD activity ($P<0.05$, Fig. 1B). Further, PFTμ increased MnSOD mRNA ($P<0.05$, Fig. 1C) and protein content ($P<0.01$, Fig. 1D). PFTα also increased MnSOD mRNA expression ($P<0.05$, Fig. 1C) and did not change the protein content. From these data we conclude that PFTμ is more capable of improving MnSOD activity and mitochondrial antioxidant system in skeletal muscle than PFTα. No consistent effects of pifithrin were observed between SS and IMF mitochondria.

3.2. mtDNA content and mitochondrial COX biogenesis

Mitochondrial content, biogenesis and enzyme activities are essential for skeletal muscle health and exercise capacity. To determine whether PFTμ or PFTα affects mitochondrial biogenesis and biosynthesis of cytochrome c oxidase, we compare mtDNA content, mitochondrial biogenesis, COX subunits and assembly proteins in skeletal muscle from PFT-treated mice. Fig. 2A showed that PFTμ increased mtDNA content ($P<0.05$). Further, PFTμ increased the mRNA expression of PGC-1β, PPARγ, NRF-1, Tfam, TFB1M, and TFB2M ($P<0.05$ or 0.01, Fig. 2B,C). However, PFTα had no significant effects on mRNA levels of NRF-1, NRF-2, Tfam, TFB1M, and TFB2M (Fig. 2C). Conversely,

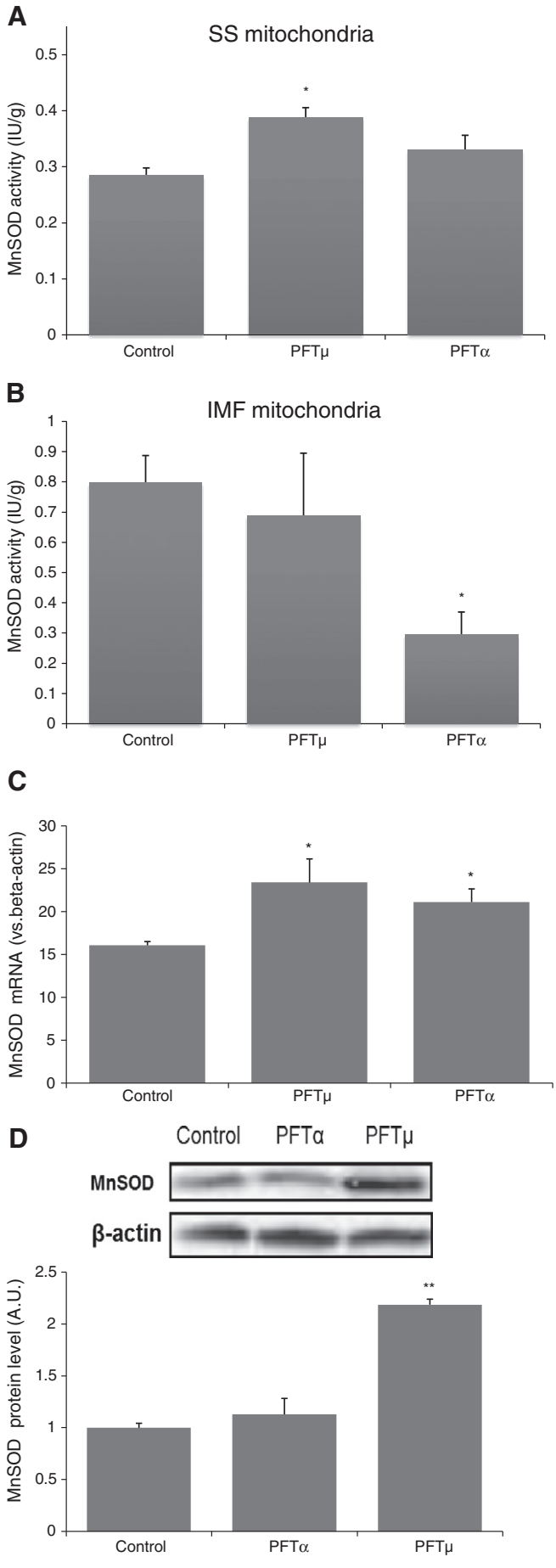

PFTα decreased the expression of PGC-1α and PGC-1β ($P<0.05$, Fig. 2B). Western blot analyses showed that PFTα decreased the protein content of PGC-1α and ERRα, and AMPKα2 phosphorylation on Thr172, whereas PFTμ did not significantly change these protein levels (Fig. 2D). As shown in Fig. 3A, PFTμ increased complex IV activity by 96% in SS mitochondria ($P<0.01$), rather than IMF mitochondria. PFTα significantly decreased complex IV activity in both mitochondrial subfractions ($P<0.01$). PFTμ increased the mRNA of SCO2 ($P<0.05$) and COX2 ($P<0.01$, Fig. 3B). Western blot demonstrated that PFTα significantly decreased the protein content of SCO (SCO1 and SCO2), an accessory protein required for assembly of the Cu(A) center of cytochrome c oxidase. PFTμ did not reduce the protein content of SCO, and significantly increased the protein content of COX4, subunit 4 of cytochrome c oxidase (Fig. 3C). As compared to PFTα, we conclude that PFTμ contributes to skeletal muscle mitochondrial biogenesis and the biosynthesis of cytochrome c oxidase.

3.3. p53 transcription activity and mitochondrial translocation

In ChIP assays, p53 that was bound to the Bax/PUMA promoter was markedly reduced in both PFTα-treated and PFTμ-treated mice (Fig. 4A,B). The mRNA expression of Bax and PUMA was also down-regulated by PFTα and PFTμ (Fig. 4D). Surprisingly, p53 that was bound to the SCO2 promoter was not affected by PFTα, and was conversely elevated by PFTμ ($P<0.01$, Fig. 4C). mRNA expression of SCO2 was also increased by PFTμ treatment ($P<0.05$, Fig. 3B). Ct values were undetectable in negative control experiments using negative primers (−ve primers) or a nonspecific antibody and in experiments where no antibody was used (Fig. S1, Tables S4–S6). These observations verify that the conditions of the ChIP assay ensured a specific assessment of the binding of p53 to its *cis*-element on the promoters. Further, endogenous mitochondrial p53 forms inhibitory complexes with protective Bcl-xL and Bcl-2 proteins, resulting in cytochrome c release from mitochondria (Endo et al., 2006). PFT-μ is a specific inhibitor of the p53–Bcl-xL interaction (Hagn et al., 2010) and directly inhibits p53 binding to mitochondria. To investigate the p53 binding to mitochondria and the direct interaction between p53 and Bcl-xL, we performed co-immunoprecipitation. Our results showed that p53 protein precipitated by Bcl-xL significantly decreased in PFTμ-treated mice and was unaltered in the PFTα-treated mice (Fig. 4E). These results indicate that PFTμ has potential effects on the p53 transcription activity, but PFTα has no effects on the mitochondrial p53 pathway in skeletal muscle.

3.4. Mitochondrial redox state and muscle mass

Fig. 5A demonstrated that PFTμ reduced the MDA level in SS mitochondria ($P<0.01$), however, PFTα increased the MDA level in IMF mitochondria ($P<0.01$, Fig. 5B). Neither PFTμ nor PFTα affected the GSH level in mitochondria. PFTμ, not PFTα, increased SOD1 mRNA ($P<0.01$, Fig. 5C) and the protein level of SOD1 ($P<0.05$, Fig. 5D). These data are consistent with reduced oxidative stress and neuroprotection using PFTμ previously reported by Nijboer et al. (2011). PFTα significantly decreased the muscle mass of EDL ($P<0.05$) and quadriceps ($P<0.01$); the antioxidant effect of PFTμ was significant and did not involve reduced muscle mass (Fig. 5E,F). We further conclude that inhibiting p53 mitochondrial translocation by PFTμ reduces mitochondrial lipid peroxidation and does not induce muscle loss in the middle-aged mice.

Fig. 1. Pifithrin-μ increases MnSOD activity in SS mitochondria. (A, B) MnSOD activity in isolated SS/IMF mitochondria, measured by a spectrophotometer ($n=7$–8). (C, D) MnSOD expression, analyzed by means of qRT-PCR ($n=8$) and Western blot. A representative immunoblot is shown for every protein ($n=4$–6). All data represent mean ± SEM. *$p<0.05$, **$p<0.01$ vs. control.

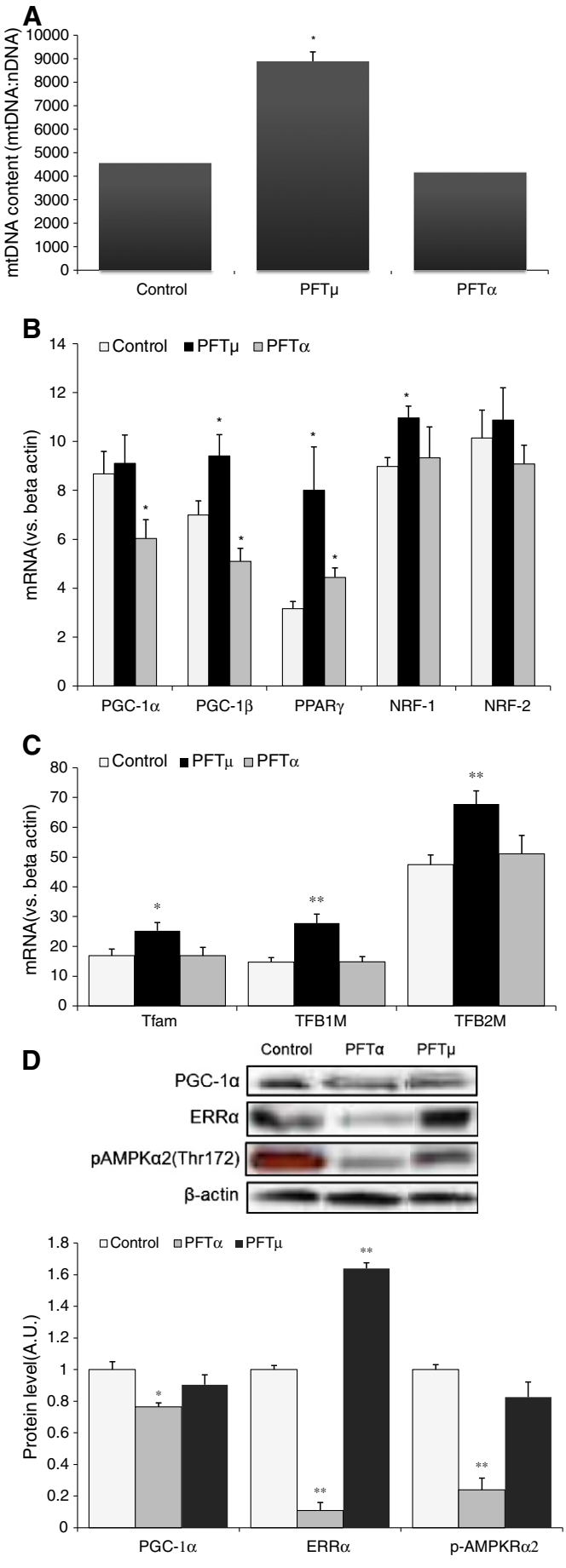

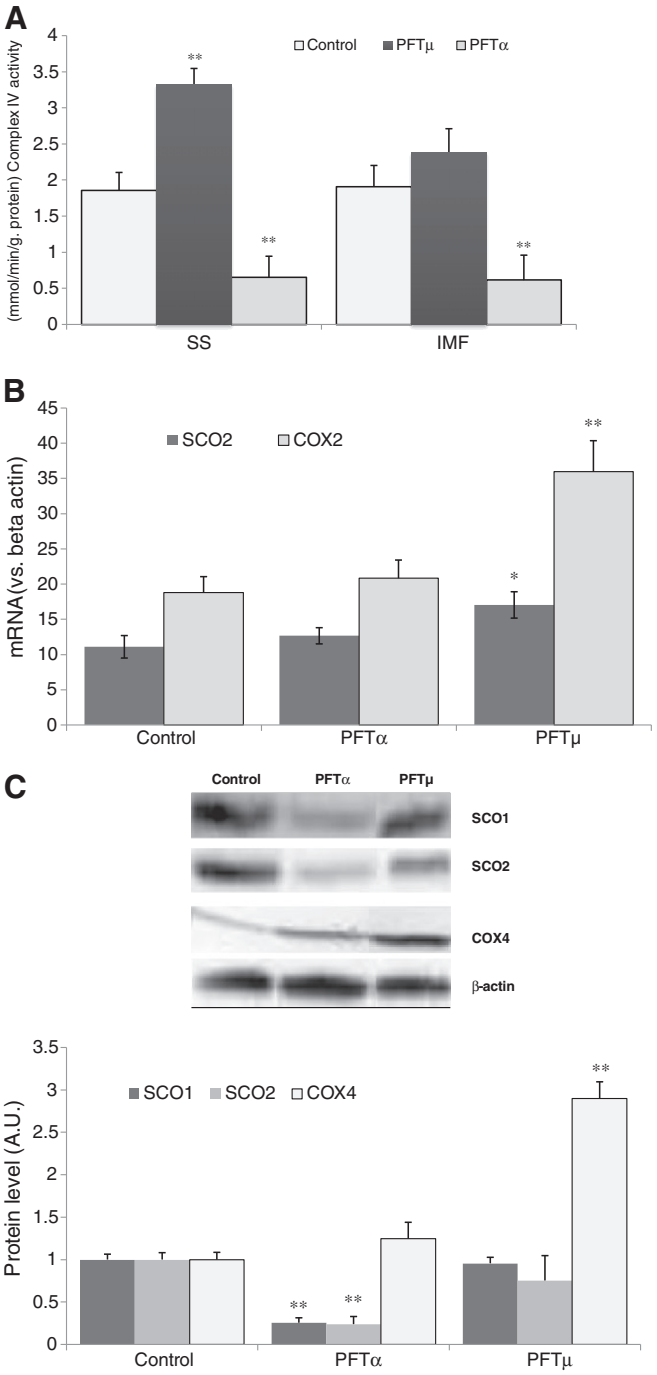

Fig. 3. Pifithrin-μ increases complex IV activity, COX4 protein content and mRNA levels of SCO2 and COX2 in skeletal muscle. (A) Complex IV activity in isolated SS/IMF mitochondria, measured by a spectrophotometer (n = 7–8). (B) mRNA levels of SCO2 and COX2, analyzed by qRT-PCR (n = 8). (C) Protein contents of COX4, SCO1, and SCO2 in skeletal muscle were analyzed by Western blot. A representative immunoblot is shown for every protein (n = 4–6). All data represent mean ± SEM. *p<0.05, **p<0.01 vs. control.

Fig. 2. Pifithrin-μ promotes mtDNA content and mitochondrial biogenesis in skeletal muscle. (A) Mitochondrial DNA content analyzed by quantitative PCR in the skeletal muscle of mice treated with pifithrin (n = 8). Data are displayed as arbitrary units relative to β-actin, a nuclear DNA marker. (B, C) PGC-1α, PGC-1β, PPARγ, NRF-1, NRF-2, TFAM, TFB1M, and TFB2M mRNAs analyzed by means of quantitative RT-PCR in the skeletal muscle of mice treated with pifithrin (n = 8). (D) Protein content of PGC-1α, ERRα and AMPKα2(p-Thr172) analyzed by Western blot in the skeletal muscle of mice treated with Pifithrin. A representative immunoblot is shown for every protein (n = 4–6). All data represent mean ± SEM. *p<0.05, **p<0.01 vs. control.

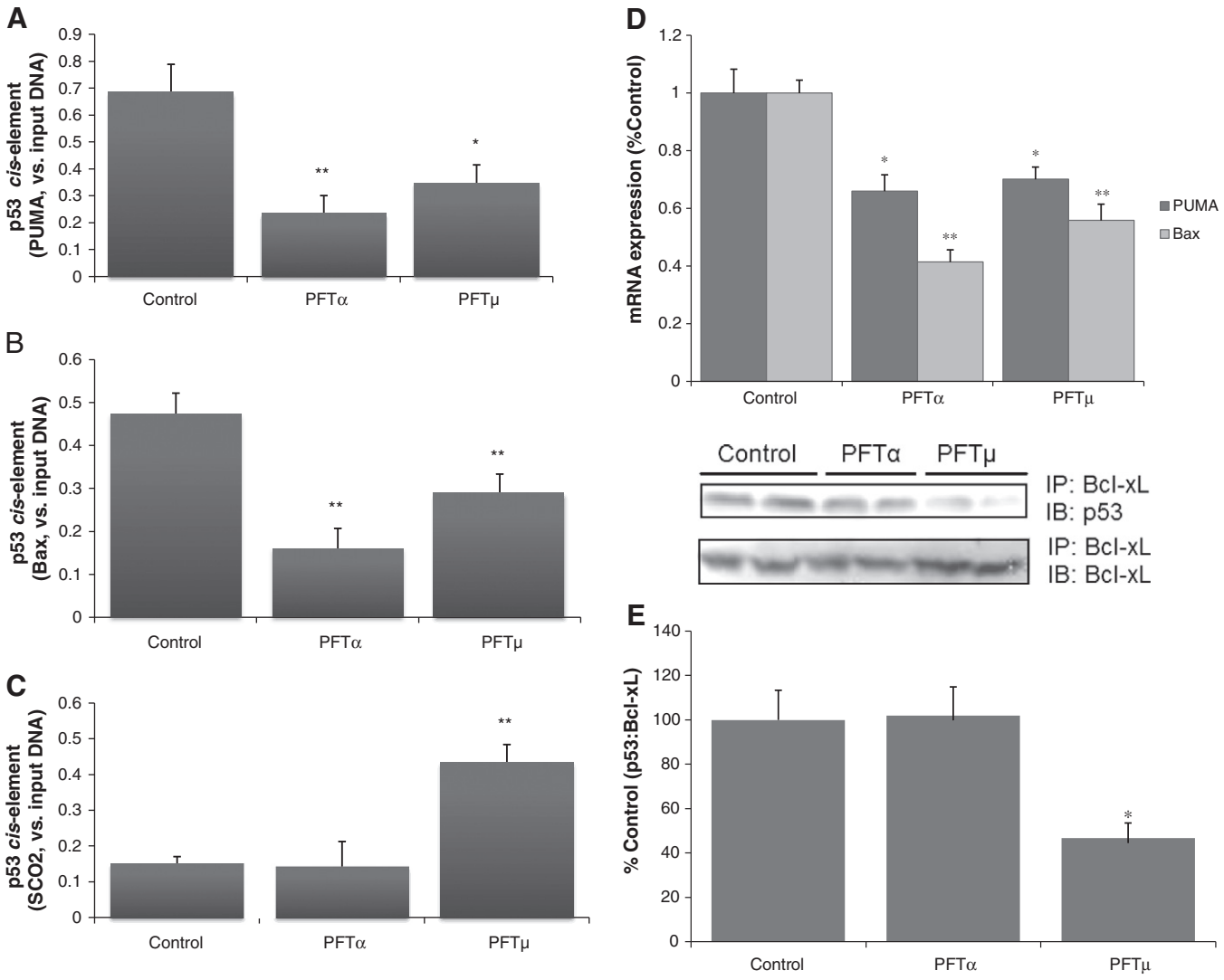

Fig. 4. Effects on p53 transcription activity and mitochondrial translocation in skeletal muscle. (A–C) The p53 *cis*-element on PUMA/Bax/SCO2 promoter, analyzed by ChIP assays and real-time PCR. Data are presented as mean ± SEM (n = 8) and displayed as arbitrary unit (A.U.) vs. input DNA. The PUMA/Bax/SCO2 promoter copies were detected by real-time PCR using + ve primers. (D) PUMA and Bax mRNAs analyzed by real-time PCR in skeletal muscle (n = 8). (E) Co-immunoprecipitation analysis of p53 immunoreactivity precipitated by Bcl-XL (n = 4). All data represent mean ± SEM. *p<0.05, **p<0.01 vs. control.

4. Discussion

We have provided evidence that PFTμ treatment of middle-aged animals prevents in vivo p53 binding to mitochondria, and increases MnSOD expression and mitochondrial COX biogenesis in skeletal muscle. However, PFTα increases oxidative stress and impairs the assembly of COX in skeletal muscle by decreasing the protein content of SCO1 and SCO2. Also, PFTα causes muscle loss in middle-aged mice. These results suggest that inhibition of the p53 mitochondrial pathway by PFTμ increases antioxidant capacity and maintains mitochondrial content and biogenesis in skeletal muscle.

4.1. MnSOD activity and SOD expressions

The major mitochondrial antioxidant system is made up of MnSOD, peroxiredoxin III, mitochondrial thioredoxin and thioredoxin reductase (Rabilloud et al., 2001). Accumulated evidence suggests that p53 plays an important role in the regulation of metabolism and intracellular redox homeostasis through transcription-dependent and -independent mechanisms. The interplay between p53 and MnSOD is an example of how nuclear and mitochondrial p53 coordinate their response to different levels of stress and contribute to the fate of cells (Sun et al., 2012). Using PFTμ and PFTα, we clearly demonstrated that the p53 mitochondrial translocation and its transcription activity were suppressed correspondingly. Interestingly, PFTμ increased MnSOD activity in SS mitochondria and did not affect MnSOD activity in IMF mitochondria. PFTα reduced MnSOD activity in IMF mitochondria, but it did not impair MnSOD activity in SS mitochondria. These results suggested a differential susceptibility of SS and IMF mitochondria in exposure to PFTμ or PFTα. In fact, SS mitochondria differ much from IMF mitochondria in many respects. Compared to the SS mitochondria, IMF mitochondria expressed a higher level of proteins associated with oxidative phosphorylation. This observation, coupled with the finding of a higher respiratory chain complex activity in IMF mitochondria (Cogswell et al., 1993), suggests a specialization of IMF mitochondria toward energy production for contractile activity (Ferreira et al., 2010). Given the relatively high proportion of IMF mitochondria within a muscle fiber, this subfraction is likely most important in inducing apoptosis when presented with ROS, ultimately leading to myonuclear decay and muscle fiber atrophy (Adhihetty et al., 2005). Anyway, PFTμ was observed to increase MnSOD activity, but PFTα decreased MnSOD activity in skeletal muscle. p53 interacted with MnSOD in the mitochondria and reduced its superoxide scavenging activity. Moreover, p53 was able to coimmunoprecipitate with MnSOD, as application of a MnSOD mimetic

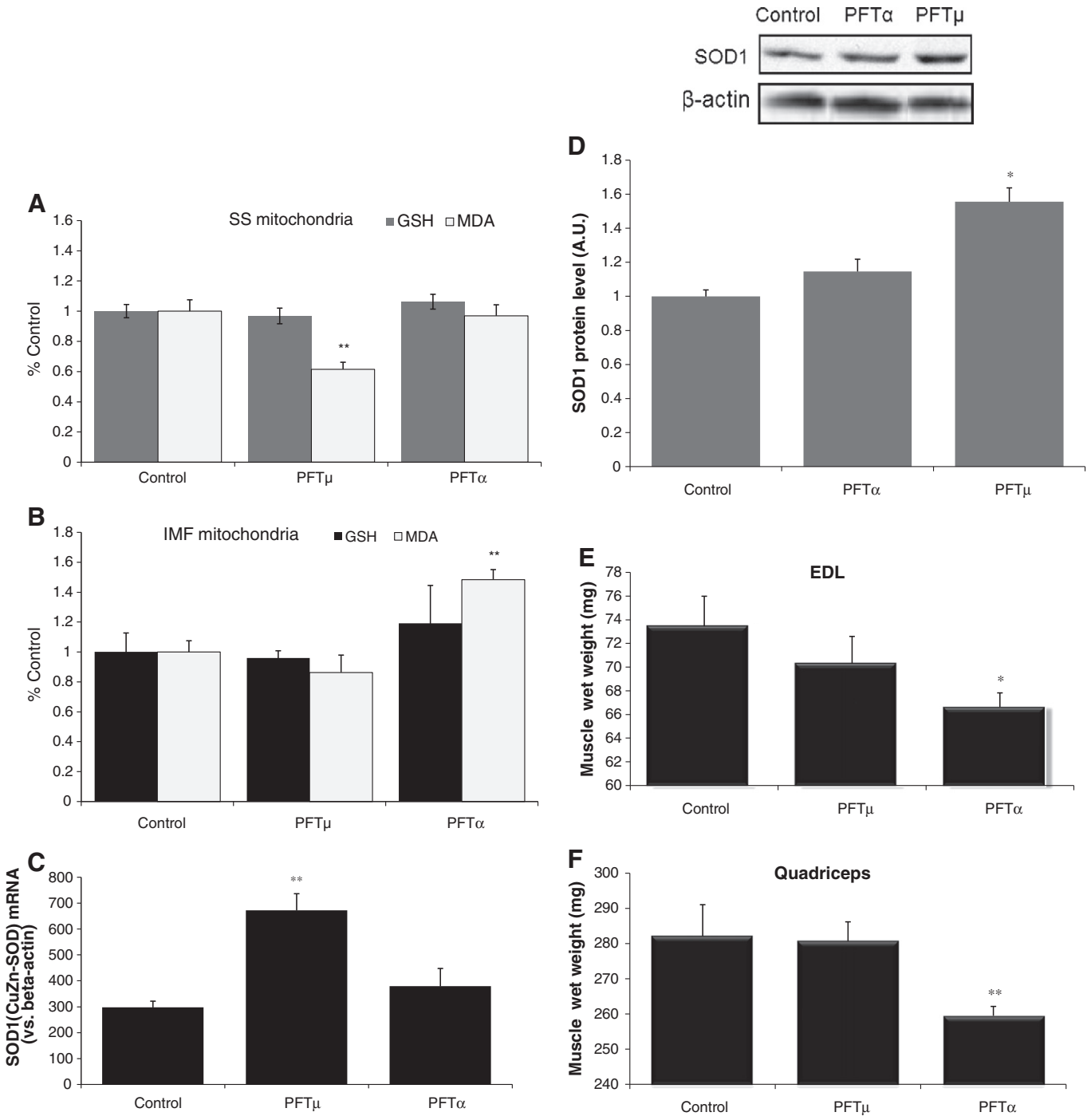

Fig. 5. Pifithrin-μ attenuates mitochondrial LPO in skeletal muscle. (A, B) MDA, GSH levels in isolated SS/IMF mitochondria, measured by a spectrophotometer (n = 7–8). (C, D) SOD1 (CuZn-SOD) mRNA level and protein content were analyzed by qRT-PCR and Western blot (n = 8). (E, F) Effects of pifithrin-μ on muscle wet weight (n = 8). All data represent mean ± SEM. *p<0.05, **p<0.01 vs. control.

(MnTE-2-PyP5 +) had only a small effect on mitochondrial localization of p53, but it completely abrogated p53 nuclear localization and expression of the p53 target gene Bax (Zhao et al., 2005). Therefore, MnSOD may bind p53 to mitochondria and further suppress p53-targeted gene transcription. The binding with p53 inhibits MnSOD superoxide scavenging activity. From our data, PFTμ that inhibits p53 mitochondrial translocation may prevent MnSOD in mitochondria from binding to p53 and thus increase MnSOD activity in mitochondria.

As a nuclear protein, p53 suppresses MnSOD promoter activity regardless of the presence or absence of putative p53 binding sites. However, a low level of p53 increased MnSOD gene transcription in the presence of the intronic-enhancer element, and this effect was dependent on NF-kappaB binding sites. p65, a subunit of NF-kappaB, could overcome the negative effect of p53 on MnSOD expression. When the level of p53 was further increased, the suppressive effect of p53 outweighed the positive effect of p65 and led to the suppression of MnSOD gene transcription (Dhar et al., 2010). Repression of MnSOD expression by p53 was dependent on the interactions of p53 with the transcription factor sp1 in the promoter of the MnSOD gene (Dhar et al., 2006). Thus, p53 plays a nonspecific and uncertain role

in MnSOD expression by interaction with the other transcription factors. p53 affects mitochondrial ROS production, in part, by regulating the expression of MnSOD and directly interacting with MnSOD to alter its activity. In turn, mitochondrial ROS affects p53 transcriptional activity and its subcellular localization, leading to a global change in cellular activity (Holley et al., 2010b). In our study, both PFTα and PFTμ increased MnSOD expression, but only PFTμ increased the MnSOD protein content. Also, we found here that expression of SOD1 was increased by PFTμ, not by PFTα. Obviously, PFTα did not function as well as PFTμ in skeletal muscle. The finding that PFTα increased oxidative stress was also found in human melanocytes (Kadekaro et al., 2012) and neonatal brain (Nijboer et al., 2011). PFTα affects neuronal cells in a dual manner. It has a protective effect at a low concentration, but becomes neurotoxic at higher concentrations (Strosznajder et al., 2005). While further work is needed to fully determine the antioxidant effects of PFTμ in multiple tissues and the dose-dependent effects, this study provides in vivo evidence that PFTμ is superior to PFTα and is able to increase superoxide scavenging activity in skeletal muscle. Accompanied by reduced MDA levels in SS mitochondria, we suggest that PFTμ improves antioxidant capacity in skeletal muscle by increasing expressions of SOD and their activities.

4.2. mtDNA content and mitochondrial COX biogenesis

To our surprise, PFTμ significantly increased mtDNA content and mitochondrial biogenesis in skeletal muscle. However, we found no change in mtDNA content in PFTα-treated mice. Almost all manipulations of p53 levels in null, heterozygous, and transgenic mice demonstrate that p53 is required for the maintenance of mitochondrial quality. p53 improved aerobic exercise capacity and augmented skeletal muscle mtDNA content. These in vivo observations were further supported by in vitro studies showing that overexpression of p53 in mouse myoblasts increases both TFAM and mtDNA levels whereas, depletion of TFAM by shRNA decreases the mtDNA content (Park et al., 2009). Loss of p53 caused mitochondrial DNA depletion and altered mitochondrial ROS homeostasis. This was accompanied by a reduction of the p53R2 subunit of ribonucleotide reductase mRNA and protein and a reduction of TFAM at the protein level only. These results elucidated mitochondria-related functions for p53 and implicated mtDNA depletion and ROS alterations (Lebedeva et al., 2009). Both of the previous studies suggested that mtDNA content was determined by the presence of the p53 gene in both cells and mice, and mtDNA depletion or increase was associated with TFAM expression.

However, overexpression and accumulation of p53 are lethal for cells and animals. p53 is located at the crossroad between cancer and aging (Papazoglu and Mills, 2007). In one hand, loss of p53 function induces tumorigenesis; on the other hand, increased p53 mediates the aging process involving enhanced apoptosis and autophagy (Ghavami et al., 2011). Moreover, the multiple roles of p53 in cells involve its intracellular distribution (Wesierska-Gadek and Schmid, 2005). Overexpression of p53 in the mitochondria reduces mtDNA abundance and increases the sensitivity of mammalian cells to exposure of nucleoside reverse transcriptase inhibitor (NRTI) by reducing mitochondrial function (Koczor et al., 2012). Mitochondrial p53 accumulation makes cells resistant to apoptosis following unrepairable DNA damage (Turinetto et al., 2010). p53 is translocated to mitochondria after mtOXPHOS inhibition (Kulawiec et al., 2009). A decline in mitochondrial function associated with compromised mtDNA quality during aging leads to a decrease in both the capacity and regulation of oxidative phosphorylation (Li et al., 2010a). The upregulation of p53 observed in aged rats contributed to the loss of outer mitochondrial membrane integrity and the mitochondrial-cytochrome c pathway of apoptosis in skeletal muscle (Tamilselvan et al., 2007). Age-related induction of p53-related genes was observed in multiple tissues. These observations support a role for the p53-mediated transcriptional program in mammalian aging (Edwards et al., 2007). p53 can arrest cell growth in response to mitochondrial p53. p53 can independently partition with endogenous nuclear and mitochondrial proteins consistent with the ability of p53 to enact senescence (Li et al., 2010b). These compelling results imply that increasing p53 with aging accumulates not only in the nucleus to target the genes involved in the aging process, but also in mitochondria to arrest cell growth and trigger apoptosis. In this study, PFTμ serves as an inhibitor to suppress p53 translocation to mitochondria since PFTμ effects on COX activity and mitochondrial biogenesis verify that p53 mitochondrial pathway has impaired mitochondrial function and biogenesis in middle-aged mice. However, PFTα reduced the protein content of PGC-1α, ERRα, and AMPKα2 phosphorylation on Thr172. This further suggests that the PFTμ effects in skeletal muscle may be more beneficial than PFTα. Presumably, PFTμ balances p53 intracellular distribution and activates mitochondrial biogenesis. It may be critical for mitochondrial biogenesis and function in skeletal muscle to prevent p53 localization in mitochondria in middle-aged mice.

SCO1 and SCO2 are copper-binding proteins involved in the assembly of mitochondrial COX, and they function not as a COX copper chaperone, but rather as a mitochondrial redox signaling molecule (Williams et al., 2005). Leary et al. (2007) suggested a mitochondrial pathway for the regulation of cellular copper content that involves signaling through SCO1 and SCO2, perhaps by their thiol redox or metal-binding state. Redox appears to be crucial to the regulation of a SCO-dependent, mitochondrial signaling pathway that modulates the rate of copper efflux from the cell. Copper efflux from the cell not only impairs complex IV activity, but also affects the activity of Cu–ZnSOD (Leary, 2010). Therefore, a potential "oxidative stress → SCO redox state → copper efflux → Cu–ZnSOD activity" pathway may be a negative feedback to maintain ROS homeostasis in the organism. Our results demonstrated that PFTμ increased complex IV activity and COX biogenesis. We also found that PFTμ increased the mRNA level of SCO2 and COX2, and protein content of COX4. Unlike PFTμ, PFTα significantly decreased the protein content of SCO1 and SCO2 in skeletal muscle, with a dramatic decrease in complex IV activity. A compelling study argues that p53 can regulate aerobic respiration via the transcriptional target SCO2 (Matoba et al., 2006). The phenotype with SCO2 deficiency, which is most severe in cardiac and skeletal muscles, is due to the loss of mtDNA-encoded COX subunits (Papadopoulou et al., 1999). Mutations in the SCO2 gene are frequently associated with mitochondrial abnormalities in skeletal muscle (Matyja et al., 2009). As such, we conclude that PFTα probably impairs the assembly of COX subunits by reducing SCO protein. Given our observation that PFTμ decreases the MDA level in SS mitochondria and increases the transcript levels of Cu–ZnSOD, mitochondrial transcription factors, and components of COX, the effects of PFTμ on skeletal muscle are likely due to increase in mitochondrial COX biogenesis and antioxidant enzymes.

4.3. p53 transcription activity and mitochondrial translocation

Surprisingly, as an inhibitor of p53 transcription activity, PFTα did not reduce SCO2 mRNA expression and p53 binding to the SCO2 promoter, but it reduced the expression of the other p53-target genes, PUMA and Bax. This finding is also similar to the data from Murphy et al. The laboratory that discovered pifithrin reported that PFTα inhibits heat shock and glucocorticoid receptor (GR) signaling but has no effect on NF-kappaB signaling. PFTα targets a factor common to all three signal transduction pathways, such as the hsp90/hsp70-based chaperone machinery (Komarova et al., 2003). However, at concentrations where PFTα blocks p53-mediated induction of p21/Waf-1 in human embryonic kidney cells, PFTα cannot inhibit GR-mediated induction of a chloramphenicol acetyl transferase reporter in LMCAT cells. The assembly of p53 or GR heterocomplexes with hsp90 and immunophilins was not affected by PFTα either in

vivo or in vitro and did not affect the nuclear translocation of either transcription factor (Murphy et al., 2004). Hence, PFTα may selectively inhibit p53 transcription activity by acting at a stage after p53 translocation to the nucleus. In the present study, PFTα suppressed the expression of PUMA and Bax, not SCO2. In other words, our finding showed that expression of p53-target genes was selectively, not specially, activated by p53.

Cell death was reduced when the p53-dependent transactivation activity was inhibited by PFTα, or PFTμ inhibited direct p53 targeting of mitochondria (Drakos et al., 2011). PUMA is a potent regulator of mitochondrial outer membrane permeabilization (MOMP), and this function is attributed to two distinct mechanisms which both rely on PUMA binding to the anti-apoptotic BCL-2 proteins: derepression and sensitization (Chipuk and Green, 2009). Consistent with this study, Fan, S et al. also found that PFTα reduced the expression of PUMA and Bax. They suggested that p53 could interfere with mitochondrial functions such as mitochondrial membrane potential via PUMA pathways, thus resulting in ROS generation (Fan et al., 2012). PUMA mediates the apoptotic signal of hypoxia/reoxygenation in cardiomyocytes through the mitochondrial pathway; inhibition of endogenous PUMA expression by PFTα repressed cardiomyocyte apoptosis (Li et al., 2011). These results suggest that PUMA cooperates with activator proteins to efficiently induce MOMP and apoptosis. Our data clearly show that even PFTμ suppresses expression of PUMA and Bax and may further reduce muscle apoptosis as well as PFTα, and the ability of PFTμ to improve mitochondrial function still remains as well. Why? Mitochondrial p53 is highly efficient in inducing the release of soluble and insoluble apoptogenic factors by severely disrupting outer and inner mitochondrial membrane integrity (Wolff et al., 2008). In vitro the mitochondrial localization of p53 is an important event in p53-dependent apoptosis (Charlot et al., 2004). The mitochondrion- and p53-mediated apoptotic pathways are responsible for the loss of fibers in age-related muscle atrophy (Dirks-Naylor and Lennon-Edwards, 2011). Thus, inhibition of p53 mitochondrial translocation by PFTμ may be critical for its beneficial effects on mitochondria and muscle mass. It is worth noting that PFTα causes muscle loss in the present study, suggesting that inhibition of transcription-dependent apoptosis by PFTα cannot prevent muscle loss during aging. Together, ChIP and Co-IP assays indicate that pifithrin affects p53 transcriptional activity and its translocation to mitochondria, and these effects thus change the expression of some genes such as PGC-1α, PGC-1β, SCO2, SOD1, and MnSOD, and activities of mitochondrial proteins such as MnSOD and TFAM. Further work is needed to fully determine how PFTμ selectively activates the p53 target gene SCO2 in skeletal muscle and how PFTμ affects MnSOD activity in mitochondria.

5. Perspectives and significance

The present study highlights a beneficial effect of PFTμ on antioxidant capacity and the biogenesis and assembly of mitochondrial COX in skeletal muscle. The most important findings were that 1) PFTμ increased mtDNA content and mitochondrial COX biogenesis in skeletal muscle, and 2) PFTμ improved mitochondrial antioxidant capacity by increasing MnSOD activity and expression of SOD1 and MnSOD. However, PFTα increased oxidative damage and decreased MnSOD activity in IMF mitochondria, and also impaired the assembly of COX in skeletal muscle by decreasing SCO proteins. This study provides in vivo evidence that p53 translocation and accumulation in mitochondria may impair mitochondrial biogenesis and its antioxidant enzymes in skeletal muscle. Although age-related muscle loss is due to apoptosis, inhibiting transcription-dependent apoptosis by PFTα caused muscle loss in the middle-aged mice. Therefore, we conclude that PFTμ, superior to PFTα, preserves muscle mass and increases mitochondrial antioxidant activity, except for its side effects.

Acknowledgments

This work was supported by grants from the National Natural Science Foundation of China (Grant Nos. 30871212, 31171142). We thank the subjects for participating in the study. We thank Qiu Linli for the kind donation of valuable tools for this study.

Appendix A. Supplementary data

Supplementary data to this article can be found online at http://dx.doi.org/10.1016/j.mito.2012.09.003.

References

Adhihetty, P.J., Ljubicic, V., Menzies, K.J., Hood, D.A., 2005. Differential susceptibility of subsarcolemmal and intermyofibrillar mitochondria to apoptotic stimuli. Am. J. Physiol. Cell Physiol. 289, C994–C1001.
Bensaad, K., Tsuruta, A., Selak, M.A., Vidal, M.N., Nakano, K., Bartrons, R., Gottlieb, E., Vousden, K.H., 2006. TIGAR, a p53-inducible regulator of glycolysis and apoptosis. Cell 126, 107–120.
Campbell, S.E., Tandon, N.N., Woldegiorgis, G., Luiken, J.J., Glatz, J.F., Bonen, A., 2004. A novel function for fatty acid translocase (FAT)/CD36: involvement in long chain fatty acid transfer into the mitochondria. J. Biol. Chem. 279, 36235–36241.
Charlot, J.F., Pretet, J.L., Haughey, C., Mougin, C., 2004. Mitochondrial translocation of p53 and mitochondrial membrane potential (Delta Psi m) dissipation are early events in staurosporine-induced apoptosis of wild type and mutated p53 epithelial cells. Apoptosis 9, 333–343.
Chipuk, J.E., Green, D.R., 2009. PUMA cooperates with direct activator proteins to promote mitochondrial outer membrane permeabilization and apoptosis. Cell Cycle 8, 2692–2696.
Cogswell, A.M., Stevens, R.J., Hood, D.A., 1993. Properties of skeletal muscle mitochondria isolated from subsarcolemmal and intermyofibrillar regions. Am. J. Physiol. 264, C383–C389.
Dhar, S.K., Xu, Y., Chen, Y., St, C.D., 2006. Specificity protein 1-dependent p53-mediated suppression of human manganese superoxide dismutase gene expression. J. Biol. Chem. 281, 21698–21709.
Dhar, S.K., Xu, Y., St, C.D., 2010. Nuclear factor kappaB- and specificity protein 1-dependent p53-mediated bi-directional regulation of the human manganese superoxide dismutase gene. J. Biol. Chem. 285, 9835–9846.
Dirks-Naylor, A.J., Lennon-Edwards, S., 2011. Cellular and molecular mechanisms of apoptosis in age-related muscle atrophy. Curr. Aging Sci. 4, 269–278.
Drake, J.C., Alway, S.E., Hollander, J.M., Williamson, D.L., 2010. AICAR treatment for 14 days normalizes obesity-induced dysregulation of TORC1 signaling and translational capacity in fasted skeletal muscle. Am. J. Physiol. Regul. Integr. Comp. Physiol. 299, R1546–R1554.
Drakos, E., Singh, R.R., Rassidakis, G.Z., Schlette, E., Li, J., Claret, F.X., Ford, R.J., Vega, F., Medeiros, L.J., 2011. Activation of the p53 pathway by the MDM2 inhibitor nutlin-3a overcomes BCL2 overexpression in a preclinical model of diffuse large B-cell lymphoma associated with t(14;18)(q32;q21). Leukemia 25, 856–867.
Edwards, M.G., Anderson, R.M., Yuan, M., Kendziorski, C.M., Weindruch, R., Prolla, T.A., 2007. Gene expression profiling of aging reveals activation of a p53-mediated transcriptional program. BMC Genomics 8, 80.
Endo, H., Saito, A., Chan, P.H., 2006. Mitochondrial translocation of p53 underlies the selective death of hippocampal CA1 neurons after global cerebral ischaemia. Biochem. Soc. Trans. 34, 1283–1286.
Fan, S., Qi, M., Yu, Y., Li, L., Yao, G., Tashiro, S., Onodera, S., Ikejima, T., 2012. P53 activation plays a crucial role in silibinin induced ROS generation via PUMA and JNK. Free Radic. Res. 46, 310–319.
Farah, I.O., Begum, R.A., Ishaque, A.B., 2007. Differential protection and transactivation of P53, P21, Bcl2, PCNA, cyclin G, and MDM2 genes in rat liver and the HepG2 cell line upon exposure to pifithrin. Biomed. Sci. Instrum. 43, 116–121.
Ferreira, R., Vitorino, R., Alves, R.M., Appell, H.J., Powers, S.K., Duarte, J.A., Amado, F., 2010. Subsarcolemmal and intermyofibrillar mitochondria proteome differences disclose functional specializations in skeletal muscle. Proteomics 10, 3142–3154.
Ghavami, S., Mutawe, M.M., Sharma, P., Yeganeh, B., McNeill, K.D., Klonisch, T., Unruh, H., Kashani, H.H., Schaafsma, D., Los, M., Halayko, A.J., 2011. Mevalonate cascade regulation of airway mesenchymal cell autophagy and apoptosis: a dual role for p53. PLoS One 6, e16523.
Grinberg, S., Teiblum, G., Rahav, G., Bakhanashvili, M., 2010. p53 in cytoplasm exerts 3′→5′ exonuclease activity with dsRNA. Cell Cycle 9, 2442–2455.
Hagn, F., Klein, C., Demmer, O., Marchenko, N., Vaseva, A., Moll, U.M., Kessler, H., 2010. BclxL changes conformation upon binding to wild-type but not mutant p53 DNA binding domain. J. Biol. Chem. 285, 3439–3450.
Holley, A.K., Dhar, S.K., St, C.D., 2010a. Manganese superoxide dismutase vs. p53: regulation of mitochondrial ROS. Mitochondrion 10, 649–661.
Holley, A.K., Dhar, S.K., St, C.D., 2010b. Manganese superoxide dismutase versus p53: the mitochondrial center. Ann. N. Y. Acad. Sci. 1201, 72–78.
Kadekaro, A.L., Chen, J., Yang, J., Chen, S., Jameson, J., Swope, V.B., Cheng, T., Kadakia, M., Abdel-Malek, Z., 2012. Alpha-melanocyte-stimulating hormone suppresses oxidative stress through a p53-mediated signaling pathway in human melanocytes. Mol. Cancer Res. 10, 778–786.

Koczor, C.A., White, R.C., Zhao, P., Zhu, L., Fields, E., Lewis, W., 2012. p53 and mitochondrial DNA: their role in mitochondrial homeostasis and toxicity of antiretrovirals. Am. J. Pathol. 180, 2276–2283.

Komarova, E.A., Neznanov, N., Komarov, P.G., Chernov, M.V., Wang, K., Gudkov, A.V., 2003. p53 inhibitor pifithrin alpha can suppress heat shock and glucocorticoid signaling pathways. J. Biol. Chem. 278, 15465–15468.

Kruse, J.P., Gu, W., 2006. p53 aerobics: the major tumor suppressor fuels your workout. Cell Metab. 4, 1–3.

Kulawiec, M., Ayyasamy, V., Singh, K.K., 2009. p53 regulates mtDNA copy number and mitocheckpoint pathway. J. Carcinog. 8, 8.

Leary, S.C., 2010. Redox regulation of SCO protein function: controlling copper at a mitochondrial crossroad. Antioxid. Redox Signal. 13, 1403–1416.

Leary, S.C., Cobine, P.A., Kaufman, B.A., Guercin, G.H., Mattman, A., Palaty, J., Lockitch, G., Winge, D.R., Rustin, P., Horvath, R., Shoubridge, E.A., 2007. The human cytochrome c oxidase assembly factors SCO1 and SCO2 have regulatory roles in the maintenance of cellular copper homeostasis. Cell Metab. 5, 9–20.

Lebedeva, M.A., Eaton, J.S., Shadel, G.S., 2009. Loss of p53 causes mitochondrial DNA depletion and altered mitochondrial reactive oxygen species homeostasis. Biochim. Biophys. Acta 1787, 328–334.

Li, S., Banck, M., Mujtaba, S., Zhou, M.M., Sugrue, M.M., Walsh, M.J., 2010a. p53-induced growth arrest is regulated by the mitochondrial SirT3 deacetylase. PLoS One 5, e10486.

Li, Y., Li, H.Z., Hu, P., Deng, J., Banoei, M.M., Sharma, L.K., Bai, Y., 2010b. Generation and bioenergetic analysis of cybrids containing mitochondrial DNA from mouse skeletal muscle during aging. Nucleic Acids Res. 38, 1913–1921.

Li, Y., Liu, X., Rong, F., 2011. PUMA mediates the apoptotic signal of hypoxia/reoxygenation in cardiomyocytes through mitochondrial pathway. Shock 35, 579–584.

Matoba, S., Kang, J.G., Patino, W.D., Wragg, A., Boehm, M., Gavrilova, O., Hurley, P.J., Bunz, F., Hwang, P.M., 2006. p53 regulates mitochondrial respiration. Science 312, 1650–1653.

Matyja, E., Pronicki, M., Kowalski, P., Czarnowska, E., Taybert, J., 2009. Remodelling of skeletal muscle cells in children with SCO2 gene mutation — ultrastructural study. Folia Neuropathol. 47, 20–32.

Mummenbrauer, T., Janus, F., Muller, B., Wiesmuller, L., Deppert, W., Grosse, F., 1996. p53 protein exhibits 3′-to-5′ exonuclease activity. Cell 85, 1089–1099.

Murphy, P.J., Galigniana, M.D., Morishima, Y., Harrell, J.M., Kwok, R.P., Ljungman, M., Pratt, W.B., 2004. Pifithrin-alpha inhibits p53 signaling after interaction of the tumor suppressor protein with hsp90 and its nuclear translocation. J. Biol. Chem. 279, 30195–30201.

Nijboer, C.H., Heijnen, C.J., van der Kooij, M.A., Zijlstra, J., van Velthoven, C.T., Culmsee, C., van Bel, F., Hagberg, H., Kavelaars, A., 2011. Targeting the p53 pathway to protect the neonatal ischemic brain. Ann. Neurol. 70, 255–264.

Pani, G., Galeotti, T., 2011. Role of MnSOD and p66shc in mitochondrial response to p53. Antioxid. Redox Signal. 15, 1715–1727.

Papadopoulou, L.C., Sue, C.M., Davidson, M.M., Tanji, K., Nishino, I., Sadlock, J.E., Krishna, S., Walker, W., Selby, J., Glerum, D.M., Coster, R.V., Lyon, G., Scalais, E., Lebel, R., Kaplan, P., Shanske, S., De Vivo, D.C., Bonilla, E., Hirano, M., DiMauro, S., Schon, E.A., 1999. Fatal infantile cardioencephalomyopathy with COX deficiency and mutations in SCO2, a COX assembly gene. Nat. Genet. 23, 333–337.

Papazoglu, C., Mills, A.A., 2007. p53: at the crossroad between cancer and ageing. J. Pathol. 211, 124–133.

Park, J.Y., Wang, P.Y., Matsumoto, T., Sung, H.J., Ma, W., Choi, J.W., Anderson, S.A., Leary, S.C., Balaban, R.S., Kang, J.G., Hwang, P.M., 2009. p53 improves aerobic exercise capacity and augments skeletal muscle mitochondrial DNA content. Circ. Res. 105 (705–712), 11–712.

Rabilloud, T., Heller, M., Rigobello, M.P., Bindoli, A., Aebersold, R., Lunardi, J., 2001. The mitochondrial antioxidant defence system and its response to oxidative stress. Proteomics 1, 1105–1110.

Ryan, M.J., Dudash, H.J., Docherty, M., Geronilla, K.B., Baker, B.A., Haff, G.G., Cutlip, R.G., Alway, S.E., 2010. Vitamin E and C supplementation reduces oxidative stress, improves antioxidant enzymes and positive muscle work in chronically loaded muscles of aged rats. Exp. Gerontol. 45, 882–895.

Saha, M.N., Jiang, H., Chang, H., 2010. Molecular mechanisms of nutlin-induced apoptosis in multiple myeloma: evidence for p53-transcription-dependent and -independent pathways. Cancer Biol. Ther. 10, 567–578.

Smith, J., Collins, M., Grobler, L.A., Magee, C.J., Ojuka, E.O., 2007. Exercise and CaMK activation both increase the binding of MEF2A to the Glut4 promoter in skeletal muscle in vivo. Am. J. Physiol. Endocrinol. Metab. 292, E413–E420.

Sohn, D., Graupner, V., Neise, D., Essmann, F., Schulze-Osthoff, K., Janicke, R.U., 2009. Pifithrin-alpha protects against DNA damage-induced apoptosis downstream of mitochondria independent of p53. Cell Death Differ. 16, 869–878.

Strosznajder, R.P., Jesko, H., Banasik, M., Tanaka, S., 2005. Effects of p53 inhibitor on survival and death of cells subjected to oxidative stress. J. Physiol. Pharmacol. 56 (Suppl. 4), 215–221.

Sun, L., Shen, W., Liu, Z., Guan, S., Liu, J., Ding, S., 2010. Endurance exercise causes mitochondrial and oxidative stress in rat liver: effects of a combination of mitochondrial targeting nutrients. Life Sci. 86, 39–44.

Sun, Y., Holley, A.K., St Clair, D.K., 2012. p53 regulation of energy metabolism and mitochondria regulation of p53 in cancer cells: an insight into the role of manganese superoxide dismutase. Curr. Pharm. Biotechnol. (Electronic publication ahead of print).

Tamilselvan, J., Jayaraman, G., Sivarajan, K., Panneerselvam, C., 2007. Age-dependent upregulation of p53 and cytochrome c release and susceptibility to apoptosis in skeletal muscle fiber of aged rats: role of carnitine and lipoic acid. Free Radic. Biol. Med. 43, 1656–1669.

Turinetto, V., Porcedda, P., Minieri, V., Orlando, L., Lantelme, E., Accomasso, L., Amoroso, A., De Marchi, M., Zannini, L., Delia, D., Giachino, C., 2010. A novel defect in mitochondrial p53 accumulation following DNA damage confers apoptosis resistance in ataxia telangiectasia and Nijmegen breakage syndrome T-cells. DNA Repair (Amst) 9, 1200–1208.

Vaseva, A.V., Marchenko, N.D., Moll, U.M., 2009. The transcription-independent mitochondrial p53 program is a major contributor to nutlin-induced apoptosis in tumor cells. Cell Cycle 8, 1711–1719.

Wesierska-Gadek, J., Schmid, G., 2005. The subcellular distribution of the p53 tumour suppressor, and organismal ageing. Cell. Mol. Biol. Lett. 10, 439–453.

Williams, J.C., Sue, C., Banting, G.S., Yang, H., Glerum, D.M., Hendrickson, W.A., Schon, E.A., 2005. Crystal structure of human SCO1: implications for redox signaling by a mitochondrial cytochrome c oxidase "assembly" protein. J. Biol. Chem. 280, 15202–15211.

Wolff, S., Erster, S., Palacios, G., Moll, U.M., 2008. p53's mitochondrial translocation and MOMP action is independent of Puma and Bax and severely disrupts mitochondrial membrane integrity. Cell Res. 18, 733–744.

Yoshida, Y., Izumi, H., Torigoe, T., Ishiguchi, H., Itoh, H., Kang, D., Kohno, K., 2003. P53 physically interacts with mitochondrial transcription factor A and differentially regulates binding to damaged DNA. Cancer Res. 63, 3729–3734.

Yoshida, Y., Holloway, G.P., Ljubicic, V., Hatta, H., Spriet, L.L., Hood, D.A., Bonen, A., 2007. Negligible direct lactate oxidation in subsarcolemmal and intermyofibrillar mitochondria obtained from red and white rat skeletal muscle. J. Physiol. 582, 1317–1335.

Zhao, Y., Chaiswing, L., Velez, J.M., Batinic-Haberle, I., Colburn, N.H., Oberley, T.D., St, C.D., 2005. p53 translocation to mitochondria precedes its nuclear translocation and targets mitochondrial oxidative defense protein–manganese superoxide dismutase. Cancer Res. 65, 3745–3750.